

A Molecular Organic Carbon Isotope Record of Miocene Climate Changes

M. Schoell, S. Schouten, J. S. Sinninghe Damsté,
J. W. de Leeuw, R. E. Summons

The difference in carbon-13 (^{13}C) contents of hopane and sterane biomarkers in the Monterey formation (Naples Beach, California) parallels the Miocene inorganic record of the change in ^{18}O ($\delta^{18}\text{O}$), reflecting the Miocene evolution from a well-mixed to a highly stratified photic zone (upper 100 meters) in the Pacific. Steranes ($\delta^{13}\text{C} = 25.4 \pm 0.7$ per mil versus the Pee Dee belemnite standard) from shallow photic-zone organisms do not change isotopically throughout the Miocene. In contrast, sulfur-bound C_{35} hopanes (likely derived from bacterial plankton living at the base of the photic zone) have systematically decreasing ^{13}C concentrations in Middle and Late Miocene samples ($\delta^{13}\text{C} = -29.5$ to -31.5 per mil), consistent with the Middle Miocene formation of a carbon dioxide-rich cold water mass at the base of the photic zone.

The Miocene marked the transition from an ice-free world with well-mixed oceans to one that was glaciated and had highly temperature-stratified oceans like those of today (1–3). Paleoenvironmental information on the Miocene Pacific is almost exclusively derived from oxygen and carbon isotope studies of foraminifera in carbonate-rich sediments from open ocean settings. Miocene sediments throughout the northern Pacific rim, however, are predominantly diatomaceous mudstones, often rich in organic matter, that are typified by the Monterey formation in California (4). Paleoclimatic data from Monterey-type sediments are sparse and limited to benthic foraminifera (5). Here we propose a new approach and show that $^{13}\text{C}/^{12}\text{C}$ ratios of organic constituents such as C_{35} hopanes and C_{27} steranes provide paleoclimatic information from Monterey-type sediments that complement paleoclimatic studies from open ocean sediments.

We examined samples from the Miocene Monterey formation at Naples Beach, California (Figs. 1 and 2 and Table 1), a Miocene section that has been the subject of many geological and geochemical studies (5–12). The time span covered in this section is from Saucian [~ 18 to 24 million years ago (Ma)] to Mohnian (≈ 8 Ma), on the basis of faunal analysis and correlations with strontium isotope data (6, 7). Total organic carbon (TOC) in these sediments ranges between 4 and 17% by weight, and organic matter is thermally immature, as indicated by sterane isomerization ratios ($20\text{S}/20\text{R} < 0.1$). The concentrations of sulfur-bound C_{27} steranes [for example, $20\text{R}-5\alpha,14\alpha,17\alpha(\text{H})$ -cholestane (I, Fig.

2)] and C_{35} hopanes [such as $22\text{R}-17\beta,21\beta(\text{H})$ -pentakishomohopane (II, Fig. 2)] change throughout the profile and are positively correlated with TOC (13–17). Free and sulfur-bound steranes vary only slightly in their ^{13}C content [$\delta^{13}\text{C} = -25.4 \pm 0.7$ per mil versus the Pee Dee belemnite standard (PDB)] and are isotopically similar to modern C_{27} sterols (-26.4 ± 0.5 per mil) in the Santa Monica Bay (18). In contrast, ^{13}C contents in sulfur-bound C_{35} hopanes decrease significantly during Middle and Late Miocene time ($\delta^{13}\text{C} = -29.5$ to -32.5 per mil). The latter biomarker $\delta^{13}\text{C}$ values are clearly independent of their abundance and are not related to TOC values; rather, they exhibit systematic trends that are possibly linked to changes in the Miocene surface ocean.

The cholestane carbon skeleton is derived from cholesterol and closely related structures that are defunctionalized during transport and diagenesis. One of the most effective pathways for steroid preservation in sediments results from the natural incorporation of sulfur (19). Cholesterol is biosynthesized predominantly by planktonic algae that today live optimally at depths of ≈ 0 to 30 m in Pacific coastal waters, as indicated by a sharp maximum in the concentration of chlorophyll-*a* at this depth (18). Zooplankton, another major source of cholesterol, graze on algae and have high carbon conver-

sion efficiencies, making their biomass isotopically similar to their food source (20, 21). Thus, the $\delta^{13}\text{C}$ of sedimentary cholesterol from all sources should approximate the average $\delta^{13}\text{C}$ value of algal carbon. In contrast, the C_{35} hopanes are derived from the bacteriohopane polyols (such as III in Fig. 2) and are compounds biosynthesized exclusively by prokaryotes (22, 23), including cyanobacteria and the heterotrophic eubacteria. The divergence of the $\delta^{13}\text{C}$ signatures for sedimentary steranes and C_{35} hopanes over the same time indicates that a carbon source not tied to algal productivity contributes significantly to the hopanoid biomarkers. Heterotrophic bacteria are unlikely because they would synthesize hopanes that are isotopically similar to, or slightly ^{13}C -enriched with respect to, primary algal photosynthate, including the steranes discussed above (20, 21).

The strongly correlated changes in the concentrations of sulfur-bound hopanes and steranes, as well as the TOC (Fig. 2), point to their common origin in the photic zone. Common modes of accumulation were likely controlled by high levels of photosynthetic productivity and aided by preservation in oxygen-depleted water columns similar to those in the modern Santa Monica and Santa Barbara basins (24). We believe that the predominant source of the C_{35} hopanes is cyanobacterial picoplankton including the prochlorophytes. Contributions from sedimentary bacteria to C_{35} hopanes in these sediments appear to be minor. This contention is supported by the absence of A-ring methylated hopanes, biomarkers for methylotrophs (25), suggesting that methane recycling was suppressed in the Monterey depositional environment (16). Also, bisnorhopane and trisnorhopane, biomarkers likely derived from bacteria that use pore water CO_2 as a carbon source (16), differ markedly from C_{35} hopanes both in abundance and ^{13}C content (14).

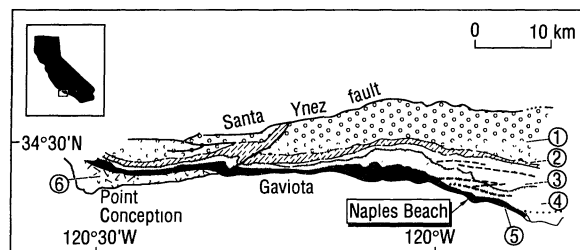
Algae and marine bacteria have different depth habitats in modern ocean water columns, a fact that holds the key to the interpretation of the Naples Beach biomarker data. Algal productivity is maximized at shallow depths (0 to 30 m), whereas bacterial biomass (*Synechococcus* and the prochlorophytes) in

M. Schoell, Chevron Petroleum Technology Company, P. O. Box 446, La Habra, CA 90633, USA.

S. Schouten, J. S. Sinninghe Damsté, J. W. de Leeuw, Division of Marine Biogeochemistry, Netherlands Institute of Sea Research, P. O. Box 59, 1790 AB, Den Burg, Texel, Netherlands.

R. E. Summons, Australian Geological Survey Organisation, GPO Box 378, Canberra ACT 2601, Australia.

Fig. 1. Map of coastal California Tertiary geology with Monterey formation and location of Naples Beach outcrop (9). The numbers in circles represent the following geological units: 1, Eocene to Upper Cretaceous marine rocks; 2, Oligocene marine rocks; 3, Oligocene nonmarine rocks; 4, Rincon shale and Vaqueros formation (lower Miocene and upper Oligocene marine); 5, Miocene Monterey formation; 6, Sisquoc formation.



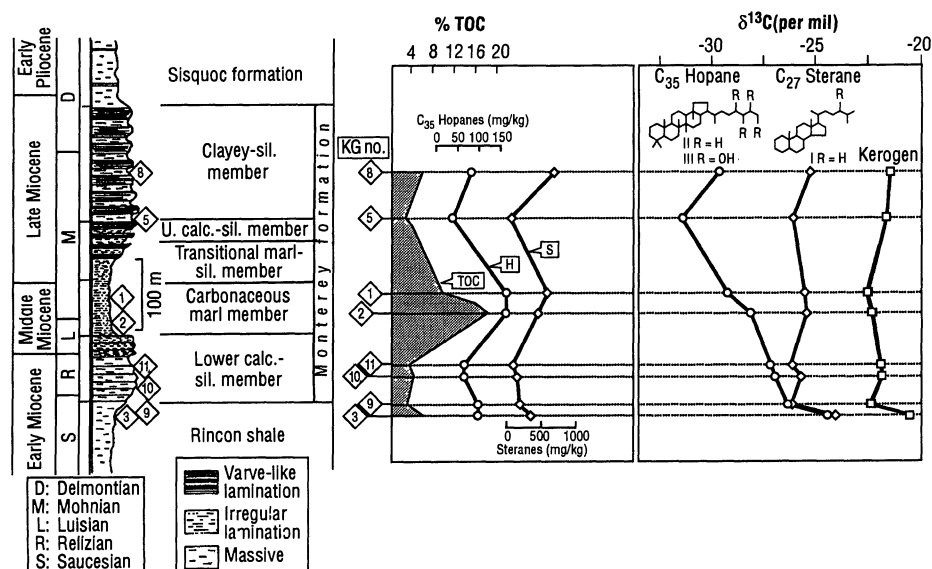


Fig. 2. Stratigraphy and lithology of the Miocene section at Naples Beach (10), depicted with the total organic carbon content (TOC) concentrations and carbon isotopic composition of macromolecularly bound C₃₅ hopane and C₂₇ sterane as well as the isotopic composition of the kerogen [kerogen data are from (12)]. The sample positions in the lithology column are schematic (for age assignments, see Table 1). Abbreviations: sil., siliceous; U., Upper; calc., calcareous.

the Atlantic Ocean occurs at all depths in the photic zone. The prochlorophytes, for example, follow the seasonally changing nitracline (26, 27). Averaged annually, about 80% of the prochlorophyte cell production occurs between 70 and 100 m [figure 9 in (26)]. The δ¹³C data for the C₃₅ hopanes in the Naples Beach profile are consistent with their origin from bacteria living at greater water depths than algae. On the basis of these considerations, we infer that the δ¹³C signatures of the C₃₅ hopanes and steranes are decoupled because of different habitat depths of their source organisms. We propose that the δ¹³C signatures of the C₃₅ hopanes reflect changes at the base of the photic zone.

The carbon isotopic composition of a polycyclic biological compound can be expressed as

$$\delta^{13}C_1 = \delta^{13}C_{DIC} - \epsilon_p - \epsilon_s \quad (1)$$

where δ¹³C_{DIC} is the isotopic composition of the dissolved CO₂; ε_p summarizes all

fractionations between dissolved CO₂ and primary photosynthate, and ε_s is the fractionation occurring during the biosynthesis of polyisoprenoids from primary photosynthate (28, 29). The isotopic difference between hopanes and steranes can be written as

$$\Delta^{13}C_{H-S} = \Delta^{13}C_{DIC} - \Delta\epsilon_p \quad (2)$$

The value for ε_s cancels out, because both biochemicals are derived from similar biosynthetic pathways with similar isotope discriminations (30, 31). The isotopic difference between steranes and hopanes (Δ¹³C_{H-S}) is then a close approximation for relative changes in the photic zone caused either by the change in δ¹³C_{DIC} or by biological fractionation. Small values of Δ¹³C_{H-S} should reflect a well-mixed photic zone and large differences should indicate a highly stratified photic zone. The value of Δ¹³C_{H-S} closely tracks the δ¹⁸O signal of Miocene foraminifera (Fig. 3B), which sug-

gests that Δ¹³C_{H-S} monitors the cooling of waters in the deep photic zone during this time.

Variations in δ¹³C_{DIC} in the photic zone (<100 m) can be caused by CO₂ removal through photosynthesis, organic matter remineralization, CO₂ exchange with the atmosphere, and the vertical or lateral transport of water masses (32, 33). The δ¹³C_{DIC} profiles through the photic zone in the Pacific change by only 1 to 1.5 per mil between water depths of 25 and 100 m (32, 33). Even in the eutrophic Santa Monica Bay, the δ¹³C_{DIC} values are ≈1.5 and ≈0.3 per mil at depths of 25 and 100 m, respectively (18). Changes of this magnitude are far too small to account for the change of 6 to 7 per mil in the ¹³C content of hopanes in the Naples Beach profile (Fig. 3). The highly productive modern Santa Monica Bay shows that high rates of algal photosynthesis alone are insufficient to affect the δ¹³C of surface ocean waters to account for the carbon isotope changes in Miocene biochemicals at Naples Beach. During the total anoxia of a water column possibly caused by exceptionally high surface productivity, one would expect a concomitant change in the δ¹³C of total organic carbon and that of coeval carbonates (34); such effects are not observed in the Naples Beach profile (5, 35).

The fractionation ε_p is the sum of all fractionations associated with (i) CO₂ transfer to the site of carboxylation, (ii) combined Rubisco carboxylation, and (iii) growth rate (29, 36). Many studies show that ε_p values correlate with the concentrations of dissolved CO₂ [CO₂(aq)] and concomitant changes in temperature (28, 37, 38). Excellent correlations between δ¹³C of particulate organic carbon (POC) and temperature have been observed in the Drake Passage where cold antarctic waters mix with mid-latitude waters (38). Cell size and growth rate, however, are important factors that can obliterate the correlation of δ¹³C_{POM} with [CO₂(aq)] (29, 36).

In the case of the Naples Beach profile, we have indirect evidence that it is mostly the changing water temperature and related changes in [CO₂(aq)] that caused the change in the isotopic composition of the hopanes and Δ¹³C_{H-S}. We used as an approximation the correlation between isotopic composition of POC and temperature in modern oceans [≈1.6°C for each per mil change in δ¹³C (38)] and the today's δ¹³C of the shallow photic zone sterols for calibration (Fig. 4). From these relations, we estimate a 3.1° to 4.3°C drop of water temperature at the base of the photic zone between the Early and Late Miocene, a reasonable estimate for ice-volume-corrected temperature changes of Mi-

Table 1. Carbon isotope analyses of steranes and hopanes from a Miocene section at Naples Beach, California. Abbreviations: L., Lower; M., Middle; n, number of analyses.

Epoch/stage/CN zone*	Sample*	Age* from (Ma)	Age* to (Ma)	C ₂₇ sterane δ ¹³ C† (per mil)	n	C ₃₅ hopane δ ¹³ C† (per mil)	n
Not determined	KG08	6.1	7	-25.3 ± 1.6	3	-29.7 ± 0.7	2
Delmontian/L. Mohnian	KG05	7	7.6	-26.0 ± 0.2	2	-31.5 ± 0.5	2
M. Miocene/CN5	KG01	13.7	15	-25.4 ± 0.7	4	-29.4 ± 0.8	2
M. Miocene/CN4	KG02	14	16	-25.5 ± 0.7	2	-28.2 ± 0.2	2
Saucesian/Relizian	KG11	17.6	17.7	-26.3 ± 0.9	3	-27.3 ± 1.5	2
Saucesian	KG10	17.6	17.7	-25.7 ± 1.0	3	-27.0 ± 0.8	2
Saucesian	KG09	17.7	24	-25.9 ± 0.4	3	-26.6 ± 0.2	2
Saucesian	KG03	17.7	24	-24.1 ± 0.2	2	-24.7 ± 0.3	3

*Sample numbers and ages are from (7). †1σ SD of repeat analyses.

ocene Pacific deep waters (39). Also, $\Delta^{13}\text{C}_{\text{H-S}}$ values for Late Miocene time lead to a lower photic zone temperature of 10° to 11°C, in good agreement with today's temperatures of 9.5° to 10.5°C at a depth of 80 to 100 m in coastal California waters (Fig. 4). These reasonable temperature estimates deduced from biomarker carbon isotopes are circumstantial evidence that the main control on $\delta^{13}\text{C}$ of these organic constituents was the concentration of dissolved CO_2 and its concomitant temperature changes.

The ^{13}C concentrations of C_{35} hopanes

and the isotopic difference between steranes and hopanes closely follow other paleoclimatic events such as the buildup of the Antarctic ice shield and the various Miocene glaciations (40–42) (Fig. 3, A and B). During the Early Miocene, dissolved CO_2 and $\delta^{13}\text{C}_{\text{DIC}}$ (and very likely temperatures) were similar throughout the photic zone, indicating well-mixed surface waters (Fig. 4). The photic zone stratification deduced from the organic isotope record at Naples Beach is in accord with the main body of Miocene paleoceanographic work that found the Pacific to have

evolved from a well-mixed water body to a highly complex temperature-stratified ocean (1–5, 40–44). The carbon isotopic signatures of biomarkers augment this picture. For example, a change in $\Delta^{13}\text{C}_{\text{H-S}}$ at 14 to 15 Ma corresponds with a major cooling event for Pacific deep waters recorded by the $\delta^{18}\text{O}$ values of benthic foraminifera (40–42) (Fig. 2B). Also, East Antarctica became permanently covered by ice during this time interval (3, 44). The $\Delta^{13}\text{C}_{\text{H-S}}$ data suggest that the trend to a more stratified photic zone continued into the Late Miocene, correlated with a series of glaciations at the boundary of Middle to Late Miocene (44). Finally, our data in Fig. 3 indicate a reversal of this trend during the Late Miocene around 7 to 8 Ma, consistent with the minor warming events observed in the deep-sea $\delta^{18}\text{O}$ record (1, 40, 41). The organic carbon isotope record suggests that the changes in the deep photic zone were closely coupled with changes of deep-water masses in the Pacific and that the shallow photic zone was not affected by these changes.

Our conclusions are partly based on a favorable comparison of Miocene data with modern eastern Pacific coastal water conditions. In our case, this comparison may be valid because we compared ancient and modern data from similar oceanographic settings. However, care must be exercised when different modern and ancient oceanographic settings are compared. Also, our assumption of an origin of C_{35} hopanes from cyanobacteria living predominantly in the deep photic zone needs confirmation from modern data. Furthermore, a calibration of sterane and hopane ^{13}C contents with modern water temperature and $[\text{CO}_2(\text{aq})]$ data would be necessary for the development of carbon isotope signatures of biomarkers as a paleoceanographic tool. Overall, however, we consider the striking parallelism of the isotopic data derived from biomarkers with known paleoclimatic events as strong circumstantial evidence in favor of their paleoceanographic significance.

Organic carbon isotope signatures of biomarkers are not affected by diagenesis as long as the basic carbon skeleton of the biological structure of the molecule is preserved. Therefore, carbon isotope analyses on steranes and hopanes could possibly advance our knowledge of the general climate changes beyond Miocene time to the geologic record. In addition, with organic compound isotope data we may be able to gain paleoclimatic information from sediments accumulating at continental margins and in epeiric seas, environments from which little paleoclimatic data is yet available.

Fig. 3. (A) The C_{27} sterane and C_{35} hopane $\delta^{13}\text{C}$ values interpreted as indicators of changing water masses in the shallow and deep photic zone during the Miocene. Modern sterols in the Santa Monica Bay synthesized at 25-m water depth and about 14°C water temperature (18) are similar to Miocene steranes in the Naples Beach section. These data suggest that shallow photic zone conditions in the Miocene were similar to those today in Pacific coastal waters. The development of the Antarctic ice sheet (2, 3) is depicted by the thickening bar at the top (not to scale) and the numbers below the bar are ages of Miocene glaciations (44). **(B)** Isotopic difference ($\Delta^{13}\text{C}_{\text{H-S}}$) between C_{27} steranes and C_{35} hopanes. The lower solid line is $\Delta^{13}\text{C}_{\text{H-S}}$ as measured. The upper solid line is $\Delta^{13}\text{C}_{\text{H-S}}$ corrected for the difference ($\delta^{13}\text{C}_{\text{DIC}}$) in the photic zone of contemporary Santa Monica Bay [$\Delta^{13}\text{C}_{\text{DIC}} \sim 1.2$ per mil (17)]. In the Early Miocene photic zone, $\Delta^{13}\text{C}_{\text{H-S}}$ likely started at the lower line (no $\Delta^{13}\text{C}_{\text{DIC}}$ gradient) and ended at the upper line in Late Miocene after a $\Delta^{13}\text{C}_{\text{DIC}}$ gradient evolved with the advent of cold waters at the base of the photic zone. The expression $\Delta^{13}\text{C}_{\text{H-S}}$ represents the residual organic isotope signal that is only related to $[\text{CO}_2(\text{aq})]$ or concomitant temperature gradients in the photic zone. The Miocene $\delta^{18}\text{O}$ record for benthic foraminifera is from (41).

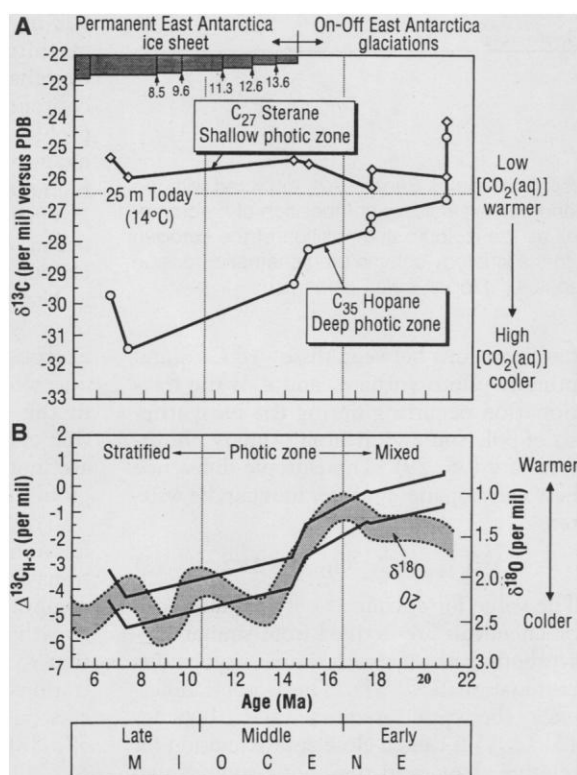
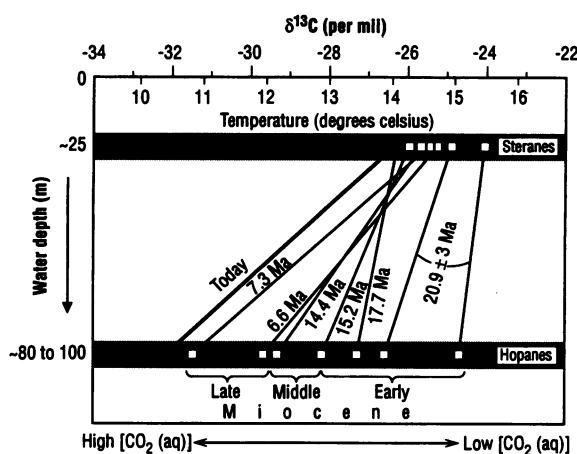


Fig. 4. Development of photic zone water-column stratification during the Miocene, reconstructed from carbon isotopic compositions of biomarkers. The C_{27} steranes and C_{35} hopanes are assumed to represent conditions in the shallow and deep photic zones, respectively. The $\delta^{13}\text{C}$ value for modern sterols is from Santa Monica Bay data [$\delta^{13}\text{C} = -26.4 \pm 0.5$ per mil at a temperature of 14°C (18)]; the deep photic zone value (~70 to 100 m) is the actual measured temperature (18). The temperature scale is calibrated with the present sterol value to represent 14°C and a change of 1.6°C for 1 per mil change in the organic $\delta^{13}\text{C}$ (38).



REFERENCES AND NOTES

1. S. M. Savin, R. G. Douglas, F. G. Stehli, *Geol. Soc. Am. Bull.* **86**, 1499 (1975).
2. J. P. Kennett, *Geol. Soc. Am. Mem.* **163**, 1 (1985).
3. K. G. Miller, M. D. Feigenson, J. D. Wright, B. M.

- Clement, *Paleoceanography* **6**, 33 (1991).
4. J. C. Ingle Jr., in *The Monterey Formation and Related Siliceous Rocks*, R. E. Garrison and R. G. Douglas, Eds. (Society of Economic Paleontologists and Mineralogists, Los Angeles, CA, 1981), pp. 159–179.
 5. B. P. Flower and J. P. Kennett, *Geology* **21**, 877 (1993).
 6. D. J. De Paolo and K. L. Finger, *Geol. Soc. Am. Bull.* **103**, 112 (1991).
 7. C. M. Isaacs et al., *U.S. Geol. Surv. Open-File Rep. 92-539-D* (1992), pp. 1–12.
 8. R. E. Garrison and R. G. Douglas, Eds., *The Monterey Formation and Related Siliceous Rocks* (Society of Economic Paleontologists and Mineralogists, Los Angeles, CA, 1981).
 9. The geologic map is from C. M. Isaacs [in (8), p. 257], who used maps from T. W. Dibblee Jr. [*Calif. Div. Mines Geol. Bull.* **186**, 1 (1966)].
 10. C. M. Isaacs, *Geol. Soc. London Spec. Publ.* **15** (1984), p. 481.
 11. _____ and J. Rullkötter, Eds., *AAPG Stud. Geol. Ser.*, in press.
 12. A. Schimmelmann et al., in (11).
 13. For detailed sample preparation procedures see (14). Before isotopic analysis, *N*-alkanes were removed by molecular sieving (5A). Carbon isotope values are reported as $\delta^{13}\text{C} = 10^3[(\text{R}_x - \text{R}_s)/\text{R}_s]$, where R = $^{13}\text{C}/^{12}\text{C}$, and x and s designate the sample and the PDB standard, respectively. Individual compound isotope analyses were performed on a GC-C-MS system (14) with some modifications of the analytical configuration and procedures (14–17).
 14. S. Schouten, M. Schoell, J. S. Sinninghe Damsté, R. E. Summons, J. W. de Leeuw, in (11).
 15. J. M. Hayes, K. H. Freeman, B. N. Popp, C. H. Hoham, *Org. Geochem.* **16**, 1115 (1990).
 16. M. Schoell, M. A. McCaffrey, F. J. Fago, J. M. Moldowan, *Geochim. Cosmochim. Acta* **56**, 1391 (1992).
 17. B. R. T. Simoneit, M. Schoell, R. F. Dias, F. R. De Aquino Neto, *ibid.* **57**, 4205 (1993).
 18. D. J. Hollander, S. G. Wakeham, J. M. Hayes, written communication.
 19. M. E. L. Kohnen, J. S. Sinninghe Damsté, J. W. de Leeuw, *Nature* **349**, 775 (1991).
 20. M. J. DeNiro and S. Epstein, *Science* **197**, 261 (1977).
 21. B. D. Fry and S. C. Wainright, *Mar. Ecol. Prog. Ser.* **76**, 149 (1991).
 22. G. Ourisson et al., *Pure Appl. Chem.* **51**, 709 (1979).
 23. M. Rohmer et al., in *Biological Markers in Sediments and Petroleum*, J. M. Moldowan et al., Eds. (Prentice-Hall, Englewood Cliffs, NJ, 1991), pp. 1–17.
 24. S. Emerson, *Geophys. Monogr. Am. Geophys. Union* **32**, 78 (1985).
 25. J. W. Collister et al., *Org. Geochem.* **19**, 265 (1992).
 26. R. O. Olson, S. W. Chrisholm, E. R. Zettler, M. Altabet, J. Dusenberry, *Deep Sea Res.* **37**, 1033 (1990).
 27. S. W. Chrisholm et al., *Arch. Microbiol.* **157**, 297 (1992).
 28. K. H. Freeman and J. M. Hayes, *Global Biogeochem. Cycles* **6**, 185 (1992).
 29. R. Goericke, J. P. Montoya, B. Fry, in *Stable Isotopes in Ecology*, K. Laijtha and B. Michener, Eds. (Blackwood Scientific, London, in press).
 30. The fractionation ϵ_s in Eq. 1 is similar but not identical. The C_{35} hopanes contain all 30 carbons of the acetate-derived squalene precursor plus five from the ribose side-chain moiety (M. Rohmer et al., *J. Chem. Soc. Chem. Commun.* **1989**, 1471 (1989)). Cholestane contains 27 carbon atoms derived exclusively from squalene. Consequently, sulfur-bound hopanes are expected to be incrementally enriched in ^{13}C because of the presence of 5/35 carbohydrate-derived carbon atoms. Because the hopanes are consistently ^{13}C -depleted with respect to steranes, the difference between the $\delta^{13}\text{C}$ signatures of steranes and hopanes tends to underestimate marginally the differences arising from factors controlling photosynthetic fractionation. Although the isotopic differences between the squalene-derived pentacyclic nucleus and the side chain of a hopane have not yet been measured, we estimate that the total effect should be on the order of 1 per mil or less.
 31. In natural populations of algae and cyanobacteria, individual sterols and hopanols have isotopic compositions similar to, or slightly depleted with respect to, those of the crude lipid fractions from which they are prepared and are depleted by 3 to 6 per mil compared to total biomass (R. E. Summons, unpublished results).
 32. P. M. Kroopnick, *Deep Sea Res.* **32**, 57 (1985).
 33. A. P. McNicol and E. R. M. Druffel, *Geochim. Cosmochim. Acta* **56**, 3589 (1992).
 34. W. Kuspert, in *Cyclic and Event Stratification*, G. Einsele and A. Seilacher, Eds. (Springer, Berlin, 1982), p. 482; D. J. Hollander et al., *Global Biogeochem. Cycles* **7**, 157 (1993).
 35. Short-term ^{13}C depletions in calcites of benthic foraminifera in the Naples Beach profile around 14 Ma [figure 1 in (5)] are on the order of 1 to 2 per mil and are related to short-term ^{13}C fluctuations in sedimentary ^{13}C (B. P. Flower, personal communication).
 36. R. Francois et al., *Global Biogeochem. Cycles* **7**, 627 (1993).
 37. G. H. Rau, T. Takahashi, D. J. Des Marais, *Nature* **341**, 516 (1989).
 38. G. H. Rau, T. Takahashi, D. J. Des Marais, C. W. Sullivan, *J. Geophys. Res.* **96**, 15131 (1991).
 39. J. D. Wright et al., *Paleoceanography* **7**, 357 (1992).
 40. S. M. Savin et al., *Mar. Micropaleontol.* **6**, 423 (1981).
 41. F. Woodruff, S. M. Savin, R. G. Douglas, *Science* **212**, 665 (1981).
 42. E. Barrera et al., *Geol. Soc. Am. Mem.* **163**, 83 (1985).
 43. S. M. Savin et al., *ibid.*, p. 49.
 44. K. G. Miller et al., *J. Geophys. Res.* **96**, 6829 (1991).
 45. We thank D. J. Hollander, S. Wakeham, and J. M. Hayes for use of unpublished data from their Santa Monica Bay study; numerous contributors of the Cooperative Monterey Organic Geochemistry Study project, in particular C. M. Isaacs and A. Schimmelmann for release of information to us before publication; and J. M. Hayes, K. H. Freeman, M. A. McCaffrey, J. P. Kennett, B. P. Flower, J. D. Wright, and R. Goericke for helpful input. Supported by a PIONEER grant (J.S.S.D.) from the Netherlands Organization for Scientific Research and by the Chevron Petroleum Technology Company, whom we thank for permission to publish. This is Netherlands Institute of Sea Research Marine Biogeochemistry contribution No. 292.

22 June 1993; accepted 23 November 1993

Deep, Zonal Subequatorial Currents

Lynne D. Talley* and Gregory C. Johnson

Large-scale, westward-extending tongues of warm (Pacific) and cold (Atlantic) water are found between 2000 and 3000 meters both north and south of the equator in the Pacific and Atlantic oceans. They are centered at 5° to 8° north and 10° to 15° south (Pacific) and 5° to 8° north and 15° to 20° south (Atlantic). They are separated in both oceans by a contrasting eastward-extending tongue, centered at about 1° to 2° south, in agreement with previous helium isotope observations (Pacific). Thus, the indicated deep tropical westward flows north and south of the equator and eastward flow near the equator may result from more general forcing than the hydrothermal forcing previously hypothesized.

The upper ocean circulation is known to be vigorous and basically east-west in orientation, but despite many years of oceanographic observation of the tropical Pacific, relatively little is known about the circulation below a depth of about 1000 m. More is known about the deep tropical Atlantic circulation because of its strong water mass signatures in temperature, salinity, oxygen, and nutrients. In the Pacific the discovery of helium tongues of hydrothermal origin has resulted in the hypothesis that the dominant large-scale tropical circulation centered at about 2500 m depth consists of westward flow in two broad bands north and south of the equator (1). Recent detailed and large-scale observations made as part of the World Ocean Circulation Experiment

(WOCE) and South Atlantic Ventilation Experiment are allowing the detailed description of the major elements of the circulation at these depths. In this report, evidence of longitudinally extensive east-west flows at these depths within 15° to 20° of the equator is presented, as indicated in the fields of temperature, salinity, and oxygen measured with unprecedented latitudinal resolution; similarity between flow patterns that have been hypothesized for the Pacific and Atlantic is demonstrated.

The existence of large-scale zonal flow at depth in the South Pacific is well known because of its hydrothermal signature. Plumes of water with high $^3\text{He}/^4\text{He}$ ratios emitted from the East Pacific Rise at 15°S (2) were observed along 125°W, 135°W, and the dateline (1, 3), in a core centered at 2500 m at 15° to 20°S. Upward motion from hydrothermal sources directly over the rise that feeds the warm, helium-rich tongue extending to the west was demonstrated by Hautala and Riser (4). The South Pacific plume is also evident in maps

L. D. Talley, Scripps Institution of Oceanography, University of California, San Diego, La Jolla, CA 92093-0230, USA.

G. C. Johnson, Pacific Marine Environmental Laboratory, National Oceanic and Atmospheric Administration, Seattle, WA 98115, USA.

*To whom correspondence should be addressed.